Yarn Diameter Measurements Using Coherent Optical Signal Processing

Vítor H. Carvalho, Paulo J. Cardoso, Michael S. Belsley, Rosa M. Vasconcelos, and Filomena O. Soares

***Abstract*—A method to measure variations in yarn diameter using coherent optical signal processing based on a single photodiode plus additional electronics is described. The approach enables us to quantify yarn irregularities associated with diameter variations which are linearly correlated with yarn mass variations. A robust method of system auto-calibration, eliminating the need for a temperature and humidity controlled environment, is also demonstrated. Two yarns that span the diameter ranges commonly used in the textile industry were used to verify the system linearity and ascertain its resolution. The results obtained have been verified using image analysis. Moreover, a diameter characterization was performed under real-world conditions for three types of yarns and a correlation with capacitive measurements is also presented. The system with sensitivity of 0.034 V/mm^2 is able to detect minute variations of yarn diameter and characterize irregularities starting at very low thresholds (commercial systems generally characterize variations of 30% or greater relative to the average value).**

***Index Terms*—Electronic instrumentation, optical sensors, signal processing, yarn diameter.**

I. Introduction

THE VARIATION in the linear mass of textile yarns is a key quality parameter in the textile industry. Yarn irregularities are generally classified as follows [1]–[3]:

- Thick places–where the local linear yarn mass is well above the average value (normally by at least 35%).
- Thin places–where the local linear yarn mass is well below the average value (normally by at least – 30%).
- Neps–for especially large local linear mass increases (at least 100%).

Yarn irregularities are usually evaluated using capacitive measurements. However, optical methods have several possible advantages including better resolution and lower sensitivity to environmental factors such as humidity or temperature. We have previously developed a coherent optical signal processing system to measure yarn hairiness [4]–[8].

Manuscript received January 23, 2008; revised April 01, 2008; accepted April 06, 2008. Current version published October 22, 2008. This work was supported in part by the Portuguese Foundation (FCT) Scholarship (BD/19028/2004). The associate editor coordinating the review of this paper and approving it for publication was Dr. M. Abedin.

V. H. Carvalho and F. O. Soares are with the Department of Industrial Electronics, Minho University, Campus de Azurém, 4800-058 Guimarães, Portugal (e-mail: vcarvalho@dei.uminho.pt; fsoares@dei.uminho.pt).

P. J. Cardoso and M. S. Belsley are with the Department of Physics, Minho University, Campus de Gualtar, 4710-057 Braga, Portugal (e-mail: pjcardoso@fisica.uminho.pt; belsley@fisica.uminho.pt).

R. M. Vasconcelos is with the Department of Textile Engineering, Minho University, Campus de Azurém, 4800-058 Guimarães, Portugal (e-mail: rosa@det.uminho.pt).

Digital Object Identifier 10.1109/JSEN.2008.2005231

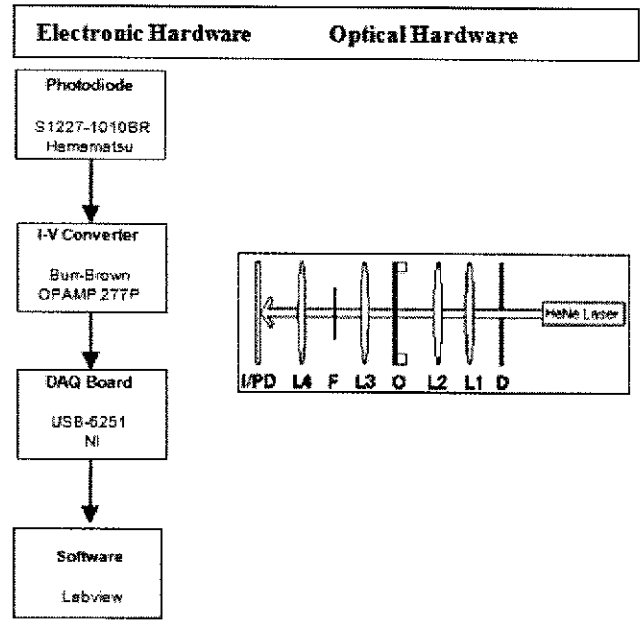

Fig. 1. Electronic and optical hardware used.

This system can be easily adapted to measure the projection of the yarn diameter along a single direction and, consequently, infer yarn irregularities. Although the system does not directly measure the yarn mass variation, a strong linear correlation exists between the yarn's diameter and mass variation. Given a high enough number of samples in a given measurement and assuming a random orientation of irregularities over the 360° around the yarn's axis, a single projection measurement should be able to adequately sample the variations in the yarn's diameter. As in the hairiness measurement, we have previously verified this expectation by simultaneously measuring the yarn's diameter along two orthogonal projections. The resulting measurements confirmed that the observed yarn diameter variations had significant statistical results for the two orthogonal directions [9].

II. Measurement System Description

The measurement of yarn diameter required an optical and an electronic setup, as illustrated in Fig. 1 [1], [4], [6].

The objective of the optical setup is to obtain the signal which is directly related to the yarn diameter in the final image plane (I) [position of the photodiode (PD) in Fig. 1]. Coherent light from a Helium Neon (HeNe) laser from Mells/Griot with 15 mW of output power, emitting at a wavelength of 632.8 nm is first spatially filtered by a diaphragm (D), to guarantee a smooth

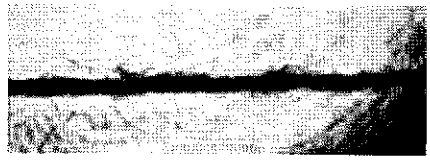

Fig. 2. Yarn image result without optical signal processing.

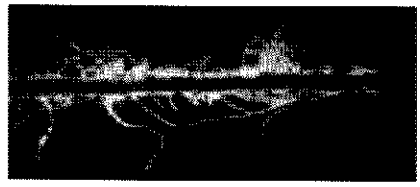

Fig. 3. Yarn image after the application of a high-pass spatial filter.

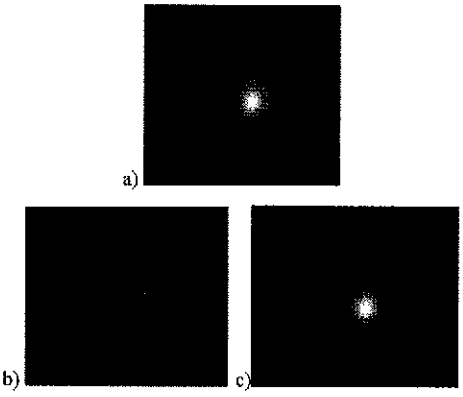

Fig. 4. Fourier plane images. (a) Without filter. (b) With a high-pass spatial filter. (c) With a low-pass spatial filter.

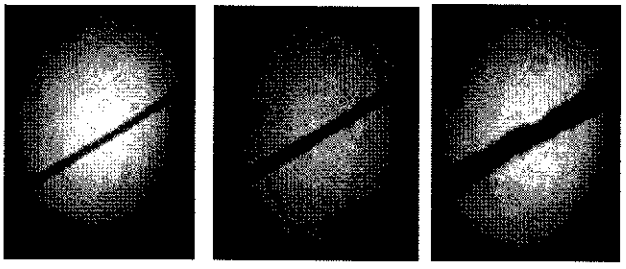

Fig. 5. Examples of images resulting from the application of the low-pass spatial filter.

transverse spatial profile, and then passed through a two plano-convex lens beam expander telescope (L1 and L2 with focal lengths of 60 mm) to produce a beam diameter of roughly 1 cm. Subsequently, the expanded beam is directed to the yarn, fixed in the object holder (O). Lens L3 forms a spatial Fourier transform of the light transmitted through the object plane at its principal focal plane (F) at a distance of 65 mm. The size of the final image is controlled by the final lens L4 with a focal length of 60 mm.

A typical image without spatial filtering is shown in Fig. 2. Looking closely at the image, in addition to the main shadow caused by the yarn core, one can identify several small protruding fibers that also block a significant fraction of the laser light.

By placing a custom fabricated spatial filter (F) in the Fourier plane of L3, we can select which spatial frequencies in the image are allowed to propagate to the detector. Previously, we employed a high-pass spatial filter consisting of a round, roughly 1 mm diameter, opaque target placed in the Fourier plane (F) that blocks all spatial frequencies below 11 mm^{-1}, corresponding to a characteristic size of 91 microns or larger in the object plane. Fortunately, there is a good separation in the characteristic length scales of the yarns. Textile yarns typically have diameters ranging from a few hundreds of a few microns up to millimeters, while the small hairs protruding from the yarn are single fibers with diameters typically less than 10 microns. So, the high-pass spatial filter removes the lowest spatial frequencies, in particular, the slowly varying background, while highlighting the sharp contours at the yarn border, as well as the protruding fibers that constitute the hairiness of the yarn. A typical image is shown in Fig. 3, in which the protruding hairs are clearly highlighted.

In this study, we wish to accomplish nearly the opposite that is to eliminate the signal from the small protruding hairs, leaving only the main shadow due to the yarn core. This can be accomplished by using a low-pass spatial filter to process the image, allowing only the lower spatial frequencies in the image to propagate to the detector plane [10]–[13]. The low-frequency spatial image is dominated by the shadow of the yarn core superposed on the relatively smooth background of the incident laser beam.

Fig. 4(a)–(c) show the intensity distribution in the Fourier plane of L3 for the above cases.

Fig. 5 presents the images of yarns with different diameters resulting from the application of a low-pass spatial filter, which is the complement of the high-pass spatial filter used in the hairiness measurements. This eliminates all spatial frequencies above 11 mm^{-1}, corresponding to a characteristic size of 91 microns or inferior in the object plane. As expected, the hairiness signal is almost completely absent.

The electronic hardware is designed to obtain a voltage that is proportional to the total optical power incident on the detector. The output of a transimpedance amplifier [14] based on a *Burr–Brown* operational amplifier (OP277P) connected to the photodiode (S1227–1010BR) from *Hamamtasu* is read by a channel of USB-6251 Data Acquisition Board (DAQ), from *National Instruments*.

Some of the main features of the operational amplifier are: ultra low offset voltage (10 μV), high open-loop gain (134 dB), high common-mode rejection (140 dB), low bias current (1 nA maximum), and a bandwidth of 1 MHz. The photodiode was chosen based on its low cost, and high sensitivity for red wavelengths (for the emitter used (Laser) – 0.39 A/W), large active measurement area (10 × 10 mm^2), low dark current (maximum of 50 pA), high shunt resistance (2 GOhm), a noise equivalent power (NEP) of 3.1×10^{-15} $W/Hz^{1/2}$, and low terminal capacitance (3000 pF). The DAQ Board is a high-resolution (16 bit) board, with high speed (maximum acquisition rate of 1.25 MS/s), high analogue input range (maximum of ±10 V) and good precision (±1 least significant bit, LSB).

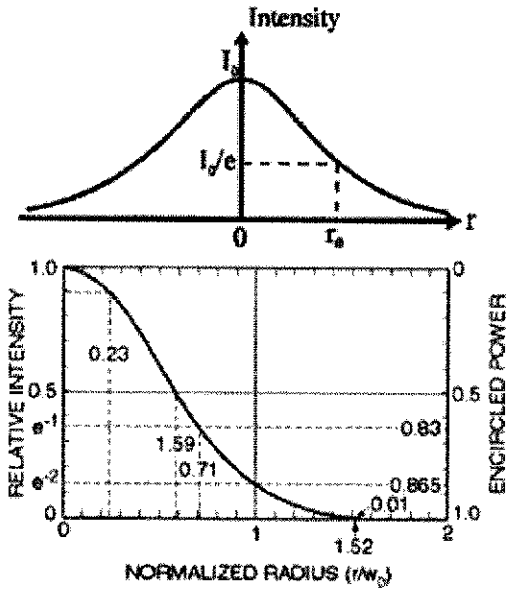

Fig. 6. A Gaussian intensity distribution typical of a HeNe laser.

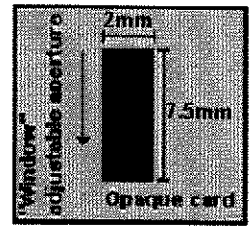

Fig. 7. Used aperture in the photodiode.

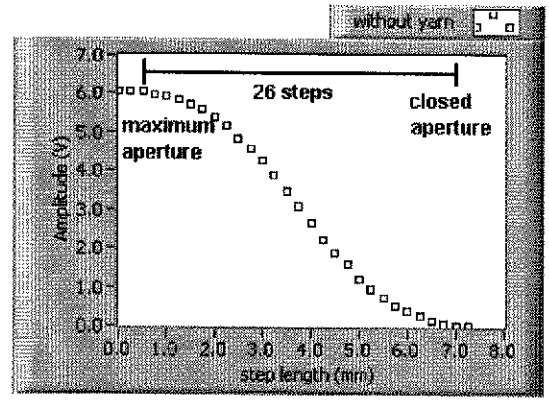

Fig. 8. Photodiode signal variation as the window aperture was varied without the presence of yarn in the object plane.

However, as the intensity of the laser light which is not blocked by the yarn, caused the photodiode to saturate, we have placed a linear polarizer, which has been adjusted to attenuate the laser light signal before the photodiode. The polarizer was adjusted so that the signal without any yarn present will still be in the linear response range of the photodiode.

III. Determination of the Yarn Diameters

A. The Gaussian Nature of the Incident Laser Beam

A difficulty in measuring yarn diameters arises from the fact that the fundamental transverse spatial mode of the HeNe laser is Gaussian in shape rather than being spatially uniform. Thus, depending on where the yarn is placed in the incident beam, more or less optical power will be blocked. The light intensity is approximately uniform near the center but decays steeply in the spatial wings. The best approximation for linearity is obtained in the centre of the beam and its close surroundings. A projection along a single dimension of a typical Gaussian intensity distribution is presented in Fig. 6 [15]–[17].

Mathematically, the Gaussian intensity distribution of the laser beam is given, as a function of the radius r by

$$I(r) = I_0 \exp\left[-\frac{2r^2}{{w_0}^2}\right] \tag{1}$$

where the parameter w_0, normally called the Gaussian beam radius, is the distance from the optical axis for which the intensity is reduced by $1/e^2$ (0.135). At $r = 0.59w_0$, the intensity drops to 50% of its maximum, while at $r = 2w_0$, the intensity is only 0.0003 of its maximum value.

In this specific approach, we consider that the yarn to be measured is positioned close to the laser beam center, called zone 1, or even due to the fluctuations in the yarn position provoked by the traction system in an adjacent zone designated zone 2. As we show in the following, if the yarn is limited to these two illumination zones, it is possible to obtain an approximate proportionality between the yarn diameter and the quantity of laser light blocked.

B. Study of Correlation Between the Laser Beam Area and the Output Voltage

1) Without Yarn: As shown in Fig. 5, the presence of yarn in the object plane will provoke a localized shadow in the image plane. Our goal is to correlate the reduction in signal caused by this shadow with the yarn diameter. To accomplish this, we need to calibrate the response variation of the photodiode to a localized change in the laser beam illumination. We carried out this calibration by placing, in front of the photodiode, a "window" with a variable aperture adjustable in steps of 250 μm using a micrometer stage to translate a movable card. Fully open, the maximum aperture has an area of 7.5 mm × 2 mm, as presented in Fig. 7.

With this construction we measured the photodiode signal over 30 different steps as the window changes from fully open to fully close. The resulting signals are displayed in Fig. 8.

Although the full aperture has a height of 7.5 mm, Fig. 8 shows that only 26 steps are necessary to go from a maximum signal to a null signal. Effectively, for steps numbered 0 and 1, the aperture did not block any of the incident laser light, since the same signal is observed as for step 3. In contrast, at step 28, the incident beam was already completely blocked by the aperture and so step 29 is redundant. In total, we need 25 steps (considering that the initial point, maximum aperture, is taken as the reference), to totally close the aperture. This means that the effective height of the illuminated area on the photodiode is between 6 and 6.25 mm.

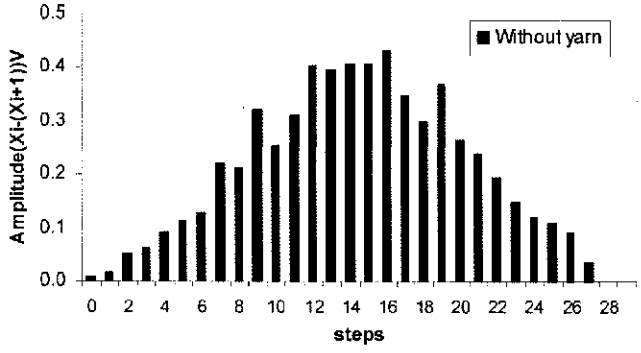

Fig. 9. Signal difference between adjacent steps.

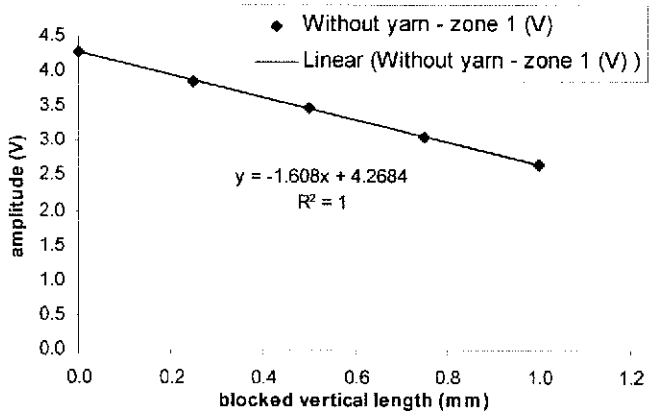

Fig. 10. Linear fit to the signal measured as the translating window passed through the zone 1 of the laser illumination.

An approximately linear variation in the signal is observed for the aperture distances ranging between 2.5 and 5 mm, which corresponds to the region of maximum laser intensity (zone 1), which is characterized for five steps. Alternatively, in Fig. 9, we display the signal difference between adjacent steps.

As expected, the curve traced out by the data of Fig. 9 is roughly a Gaussian distribution. The center steps, between 12 and 16, produce an almost constant variation in signal and can be identified as corresponding to illumination zone 1 (Fig. 10). The extension of zone 1 to the two adjacent steps (10; 11; 17; 18) is identified as zone 2.

The nearly constant variation of the signal in zone 1 gives rise to a very linear variation in the signal amplitude as a function of the blocked vertical distance, as displayed in Fig. 10.

We note that the regression correlation coefficient R^2 value of the linear least squared fit is the unity (one). Using the slope of the least squared fit, we can quickly estimate the sensitivity of the system. For the specific optical and electronic hardware configuration used, a vertical window reduction of 1 mm, corresponding to 2 mm^2 of illumination area, reduces the signal by 1.608 V. Taking into account the optical reduction factor of 66% relative to the object plane, a object which causes a variation of $2mm^2$ in the image plane would have an actual area of $4.59mm^2$ yielding an overall system sensitivity of $0.350\ V/mm^2$.

To carry out continuous measurements, the yarn would have to be translated through the object plane using some kind of traction system. This could provoke some small deviations of the

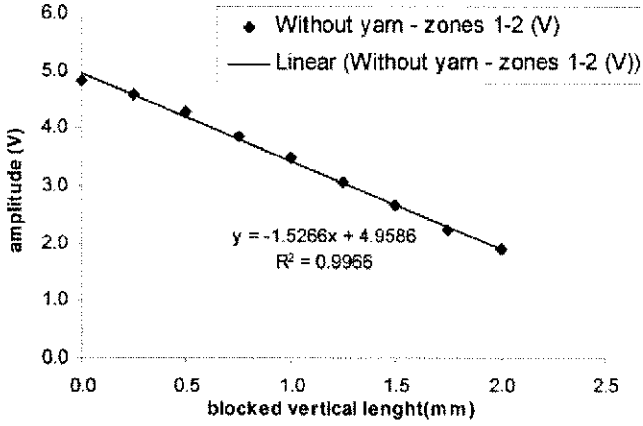

Fig. 11. Signal variation over zones 1 and 2 from Fig. 10.

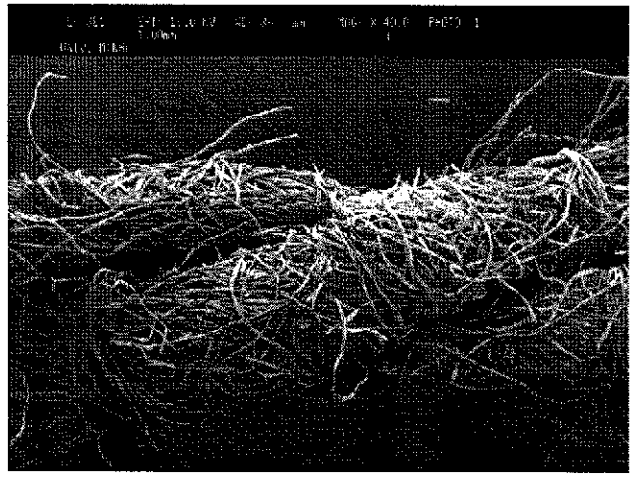

Fig. 12. Electron microscope picture of the thicker yarn.

yarn from the exact center of the laser beam illumination. To study the influence of such deviations, we have also analyzed the variation in signal that is obtained considering zones 1 and 2. Fig. 11 presents the corresponding data together with the linear least squares fit. The overall fit is still quite acceptable. The difference in best fit slopes between Figs. 10 and 11 is less than 6%, suggesting that even if the yarn moves by as much as $+/-2$ mm in the object plane (corresponding to less than $+/-1.3$ mm in the image plane) this will provoke an uncertainty in the diameter measurements of less than 6%.

2) Considering Two Different Yarns Diameter: To measure yarns diameters, we have repeated the above procedure of closing the window aperture across the detector, with the presence of yarn in the object plane. Two different yarns that span the range of diameters typically used in the textile industry were analyzed. In each case, the yarn under study was oriented parallel to the direction of the window aperture.

Fig. 12 shows an electron microscope image of the thicker yarn (295 g/km of linear mass). This yarn has a diameter that varies from 0.99 to 1.22 mm with a twist step of around 2 mm.

The ratio of the signal obtained with yarn to that obtained without yarn over the variable aperture within the illuminated zones 1 and 2. The results are shown in Fig. 13.

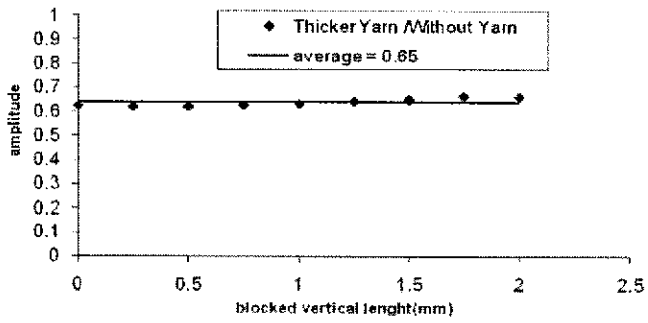

Fig. 13. Correlation between the signals registered with the thicker yarn and without yarn.

The points of Fig. 13 show that there is an almost constant ratio between the signals with and without the thicker yarn in the object plane. The slight variations observed are probably due to the variations in the yarn diameter along the length of yarn blocked in each step. The electron microscope image shows variations in diameter ranging from 0.99 to 1.22 mm, a range of 22%. If we take the average ratio of approximately 0.65 in Fig. 13, then the yarn blocks roughly 35% of the incident light. This implies that the tested yarn has an effective average diameter of (0.35∗2 mm/0.66), or 1.06 mm, close to the lower end of the range of values registered in the electron microscope image.

We note that if the yarn is not completely opaque to the incident laser light, some signal would be seen even in the shadow of the yarn core. This means that the value estimates of the absolute yarn diameter from the above relations would be slightly low. In order to obtain a valid absolute diameter measurement, we would need to consider the opacity of a given yarn, which goes beyond the objectives of the present study. However, a partial opacity would result in a nearly constant multiplicative correction factor and the registered signals should still give a reliable indication of the variations in the yarn diameter as compared with the average diameter which is the value usually quoted in textile applications.

We have repeated the above measurements for a thin yarn (4.2 g/km of linear mass). In doing so it was possible to characterize the resolution limits of the method presented.

Fig. 14 shows an electron microscope image of the thinner yarn. From this image, it is determined that the diameter varies between 0.103 and 0.147 mm with a twist step around 0.384 mm.

On average, the signal reduction due to the shadow of the thin yarn is only 0.1561 V/mm of yarn, which results in an overall sensitivity of 0.034 V/mm^2 in the object plane. Using these results we can characterize the system resolution.

At the final points in zone 2, the system has problems in detecting variations in illumination. At this point, we have an aperture 2 mm wide (zones 1 and 2) and a yarn whose diameter projected in the image plane varies between 68 μm [0.103 mm (minimum electron microscope yarn diameter) ∗0.66 (optical amplification)] and 97 μm [0.147 mm ∗ 0.66]. So, if the yarn was completely opaque to the laser light within its diameter, we should have a blocked area which may vary between 0.136mm^2 (68 μm ∗ 2 mm) to 0.194 mm^2 (97 μm ∗ 2 mm). These small

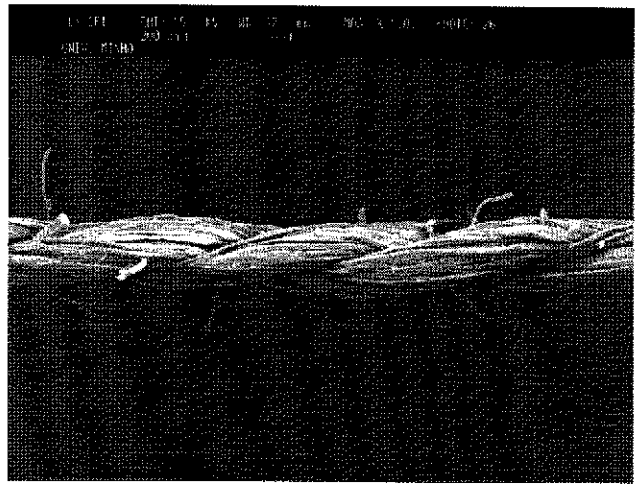

Fig. 14. Electron microscope picture of the thinner yarn.

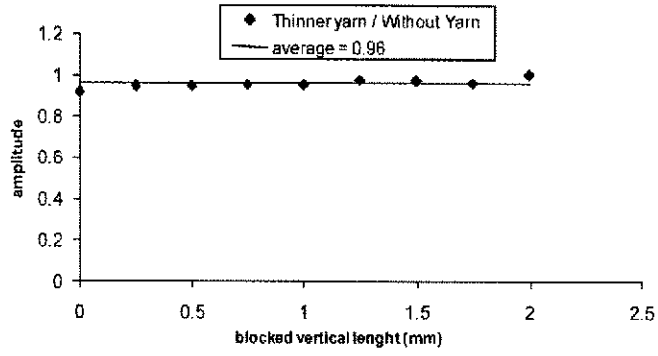

Fig. 15. Relationship between thinner yarn signal and without yarn signal.

estimated areas are further reduced by the finite opacity of the yarn and towards the limits of zone 2 we rapidly reach a situation in which the present system is not capable of detecting the important variations. However, this is a limitation which does not occur in zone 1 (area where the yarn should be mainly located during a test), but in the limit points of zones 2. Even so, with this level of resolution located at zone 2, we are able to reliably determine the most common irregularities in textile industry as they consider at least 30% variations.

The ratio of the signal with the thinner yarn to that without any yarn present is shown in Fig. 15 as a function of the blocked vertical length of the aperture.

The ratio is roughly constant as expected at least for blocked vertical lengths up to 2 mm. Beyond this point the signal with the thinner yarn present is very close to that without yarn for these points, our measurements are essentially limited by the system resolution as referred above and we cannot perform a reliable measurement. Nevertheless, the system has a resolution significantly better than most commercial systems available on the market [18], [19]. As a general rule, they can only characterize yarns with a linear mass above 12 g/km. The thinner yarn used in this study has a linear mass of 4.2 g/km which is significantly less. Considering the average result of approximately 0.96, it implies that the yarn blocks a fraction 0.04 of the incident light, giving an effective average diameter for the tested

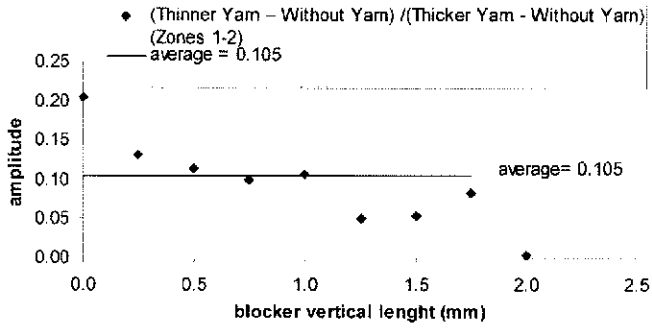

Fig. 16. Ratio of the signal blocked by the thinner yarn compared with that blocked by the thicker yarn.

TABLE I
CORRELATION BETWEEN DIAMETER RANGES OF THE TESTED YARNS

	Maximum diameter	Minimum diameter	Average
Thicker Yarn	1.22 mm	0.99 mm	---
Thinner Yarn	0.147 mm	0.103 mm	---
Thinner Yarn / Thicker Yarn	**0.120**	**0.104**	**0.112**

yarn of $(0.04 * 2\ \mathrm{mm}/0.66)$, or 0.12 mm, quite close quantification to the average diameter obtained from the electron microscope image.

C. *Study of Correlation Between Results Without Yarn and With Yarn*

As a final study, we look at the correlation between the signals blocked by the thinner yarn and the thicker yarn. The ratios of the signals (Thinner Yarn – Without Yarn) to (Thicker Yarn – Without Yarn) for zones 1 and 2 are presented in Fig. 16.

Once again, we only look at the signals corresponding to the illumination zones 1 and 2 (overall a vertical distance of 2 mm), since, as we have shown previously, in this range the signal blocked by the thinner yarn can be clearly distinguished. The average ratio obtained for the points from 0 to 1.75 mm is 0.105 with a standard deviation of 0.05. We have neglected the 2 mm value because its result is almost 0 and so, no information is obtained. This value is consistent with the expected one based on the electronic microscope images of Figs. 12 and 14. The extreme limits of the diameters in these images are presented in Table I. The value found from the data in Fig. 16 is close to the lower limit of the diameter ratio predicted from the electron microscope images. However, this value may be affected by different mean opacities for the two yarns tested. Thinner yarns show lower opacities.

IV. METHODS OF AUTO-CALIBRATION, DIAMETER DETERMINATION AND IRREGULARITIES CLASSIFICATION

Based on the above tests, we have developed a reliable robust method of system auto-calibration in order to determine the yarn diameters correctly, as well as classify irregularities without the need of a conditioned atmosphere. The following procedures were used:

a) measure the signal without yarn (Vsf) (V);
b) measure for various samples the signal with yarn (Vcf) (V);
c) determine the average of signal with yarn (Vcfa) (V), which considers the average diameter;
d) calculate the average signal blocked by the yarn ($\mathrm{Vf} = \mathrm{Vsf} - \mathrm{Vcfa}$) (V);
e) then using the theoretical relation for the yarn diameter based on the linear mass ($\mathrm{tex} = \mathrm{g/km}$), $\mathrm{d(mm)} = 4.44 \times 10^{-2} * \sqrt{(\mathrm{tex(yarn\ linear\ mass(g/km))}/\rho)}$ [20] and considering the sample length (sl) of the system (mm), we can estimate the average area blocked by the yarn, $\mathrm{Afsj} = \mathrm{sl} * \mathrm{d}\ (\mathrm{mm}^2)$;
f) determine the attenuation sensitivity for the tested yarn ($\mathrm{Sa} = \mathrm{Vf/Afsj}\ (\mathrm{V/mm}^2)$.

The algorithm starts by obtaining the system output voltage without yarn (step a). Afterwards, considering several yarn samples, it is determined the average system output voltage with yarn (steps b and c). Using these two results it is determined the average voltage signal blocked by the yarn (step d). Subsequently, calculating the theoretical yarn diameter using the yarn linear mass and considering the system sample length, it is determined the average area blocked at each sample of the yarn (step e). Finally, the relationship between steps d and e, enables the determination of the system sensitivity (step f).

After the calibration process described in the previous algorithm, the yarn diameter in each sample is determined by the following procedure:

g) determine the area blocked by each yarn sample [$\mathrm{Ai} = (\mathrm{Vsf} - \mathrm{Vcf})/\mathrm{Sa}\ (\mathrm{mm}^2)$];
h) determine the diameter in each yarn sample [$\mathrm{di} = \mathrm{Ai/sl}$ (mm)].

This procedure determines the yarn area blocked at each sample by establishing the difference between the voltage without yarn and the voltage with yarn and divided by the system sensitivity (step g). The yarn diameter at each sample is calculated as the ratio between step g and the system sample length (step h).

So, if we calculate the average diameter, we are able to determine yarn irregularities by estimating the percentage variation in diameter of each sample with reference to the average diameter.

However, if we just want to characterize yarn irregularities, we can use a simpler five steps process:

a) measure the signal without yarn (Vsf);

b) measure the signal of each sample with yarn (Vcf);

c) determine the average for all the measured samples (Vcfa);

d) determine the reference ($\mathrm{Vr} = \mathrm{Vsf} - \mathrm{Vcfa}$);

e) determine the percentage variation of each sample with yarn ($\mathrm{di\%} = 100 * (\mathrm{Vsf} - \mathrm{Vcf})/\mathrm{Vr}$).

This less complex procedure determines the difference between the signal without yarn (step a) and the average acquisition result of the samples with yarn (steps b and c), establishing the system reference (0% of diameter variation) (step d). The diameter variation to the system reference is calculated to each

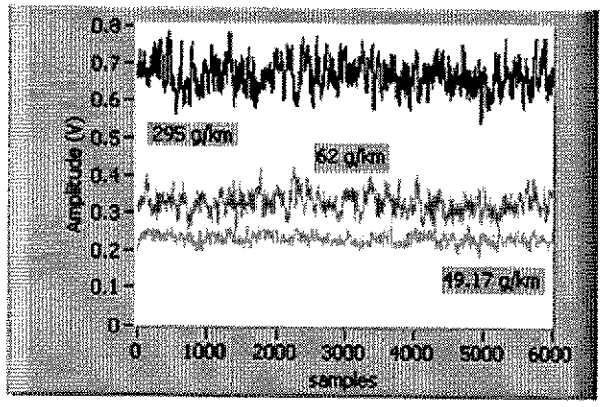

Fig. 17. Yarn blocked signals for each analyzed yarn.

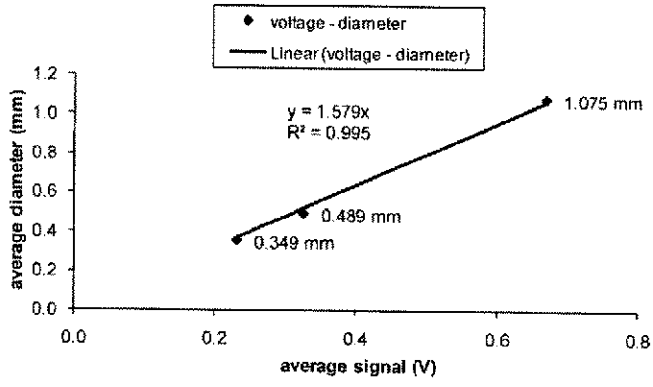

Fig. 18. Linear distribution of the system yarn diameter characterization.

TABLE II
RELATIONSHIP BETWEEN YARN DIAMETERS AND AVERAGE SIGNALS

Yarn linear mass (g/km)	Average signal (V)	Maximum diameter (mm)	Minimum diameter (mm)
49.17	0.2320	0.384	0.314
62.00	0.3265	0.518	0.460
295.00	0.6687	1.210	0.940

yarn sample as the ratio between the voltage signal blocked at each yarn sample and the system reference (step e).

V. REAL WORD CHARACTERIZATION RESULTS

A. Diameter Characterization

Three 100% cotton yarns with different linear masses of 49.17, 62.00, and 295 g/km were analyzed.

To ensure a 1 mm analysis, a window aperture, in the photodiode, with an area of 1 mm $*$ 4 mm, was built. However, as the optical hardware produced a reduction of 44% in the image plane, a 1 mm high window in the image plan corresponds to an effective height of 1 mm/0.66 = 1.52 mm in the object plane. A 4 mm wide window was used, to allow for a possible oscillation of the sample yarn. However, the yarn position was very stable, and it can be said that a high percentage of samples were acquired in the center of the laser beam where the window was placed, allowing reliable measurements (laser zone with high linearity).

We acquired 6000 samples in steps of 1 mm for each yarn. The value for calibration corresponding to the signal without yarn was 2.63 V. Afterwards, the difference between the acquisition signal and the reference value was calculated, in order to obtain the effective signal blocked by the yarn. Fig. 17 shows, as expected, that higher linear mass yarns and, consequently, larger diameter yarns, produce a greater amount of blocked signal.

Table II presents the maximum and minimum diameters of each yarn analyzed as determined using images from an electron microscope and the average value of their blocked signals.

As stated before and now confirmed by Table II, yarn linear masses are correlated with the yarn diameter. Furthermore, Table II, also shows that the average signal obtained is directly proportionality to the yarn diameter.

Fig. 18 presents the median diameter as a function of the average signal voltage for each yarn.

There is a clear tendency for a linear relationship between yarn diameter and the average signal blocked by the yarns under test, with the least squares linear fit having an R squared value very close to one (0.995).

Although a window of 4 mm instead of 2 mm was used for the online measurements, the results are still consistent. We introduced a 4 mm window to allow the possibility of higher fluctuations in the yarn position. This also provokes a larger background level resulting in a higher noise in comparison with the 2 mm window. Nevertheless, the results remain coherent, as it is clearly identified a linear variation between yarn diameter and output voltage.

B. Capacitive Analysis Versus Optical Analysis

To test the correlation between yarn mass variation and yarn diameter variation, we have measured the variation relative to the mean value of the 295 g/km yarn, using a capacitive mass variation analysis system and compared the results with the optical diameter analysis described in this study, using samples of 1 mm [21]. We used two different sections of the same yarn, so although we do not expect identical results, the measured level of variation should be similar [22]. A descriptive analysis and correlations between the two methodologies results performed with the statistical analysis software SPSS [23] is presented in Table III. There it can be observed that the values are in close agreement. Moreover, the correlation is significant at a 0.05% level. So, as expected these results confirm the statistical significance between both technologies [22].

VI. CONCLUSION AND FUTURE WORK

Considering the results obtained, it was possible to establish a direct relationship between the output system value and the yarn diameter when positioned in the laser beam zones 1 and 2. These zones are characterized by an almost constant light intensity, enabling a proportional signal variation. The diameter measurements obtained by the developed system were validated by comparison with electron microscope yarn diameter measurements.

The results used in this study depended on identifying a central illumination zone. The ideal situation would have been

TABLE III
SPSS DESCRIPTIVE ANALYSIS RESULTS

	Range (%)	Minimum (%)	Maximum (%)	Mean (%)	Mean SD error	Inter-quartile Range (%)	Covariance (%)
Optical	27.81	-14.00	13.81	0.17	0.15	6.58	25.37
Capacitive	26.82	-13.47	13.35	0.03	0.13	5.33	19.02

to induce a full saturation of the detector over its surface, which would increase the measurements precision, provided the opacity of yarns. Moreover, as this method does not rely on the coherence property of the light source, it could be generalized to other different sources, as a conventional incoherent light source as a LED. However, the measurements would then include the signal blocked by the small protruding fibers from the yarn core (hairiness), as an incoherent illumination would not allow the use of the low-pass spatial filter, introducing high spatial frequencies in the measurement (hairiness frequencies).

Additionally, the system resolution measurement is also dependent, on the amplification factor of the optical system. The system used above had a reduction factor of 0.66 between the object (yarn) plane and image (detector) plane. This led to a decrease in the measurement precision as a result of the lower blocked shadow area of the yarn. However, the system noise will not have an important influence on the system measurement, as the signal-to-noise ratio (SNR) can be adjusted easily, by reducing the active area of the measurement in order to suppress those drawbacks. Moreover, the quantification of yarn irregularities is easily achieved, considering the sample-by-sample diameter results, in order to the average diameter variation. Furthermore, a noncontrolled environment could be used as the system is able of auto-calibration.

Therefore, we can conclude that the developed diameter measurement system, based on coherent optical signal processing, is a convenient method to reliably quantify diameter variations for a large range of yarn linear masses.

In future work, we plan to combine the present diameter measurement system with the hairiness characterization system, using a single laser source together with a beam splitter positioned before the Fourier filter. The electronic hardware will also be duplicated. For higher precision diameter measurements, a photodiode linear array could be employed to obtain signals that would be equivalent to a single line cut perpendicular to the yarn in the images of Fig. 5 However, this would require more sophisticated electronic hardware, higher costs, and significantly greater computational effort for the analysis.

REFERENCES

[1] V. Carvalho, "Parametrização de Fio Têxtil Baseada na Análise de Massa," M.Sc., Minho Univ., Guimarães, Portugal, 2002.

[2] R. Furter, *Evenness Testing in Yarn Production: Part I*. Manchester, U.K.: The Textile Institute and Zellweger Uster AG, 1982.

[3] J. S. Neves, *Irregularidade dos Fios Têxteis, sua Origem, Medição e Análise*. Oporto: Author Edition, 1968.

[4] V. Carvalho, P. Cardoso, M. Belsley, R. Vasconcelos, and F. Soares, "Determination of yarn hairiness using optical sensors," presented at the EUROSENSORS XX, Gothenburg, Sweden, Sep. 17–19, 2006.

[5] V. Carvalho, P. Cardoso, M. Belsley, R. Vasconcelos, and F. Soares, "Development of a yarn evenness measurement and hairiness analysis system," presented at the IECON06, Paris, France, Nov. 7–10, 2006.

[6] V. Carvalho, P. Cardoso, M. Belsley, R. Vasconcelos, and F. Soares, "Yarn hairiness parameterization using a coherent signal processing technique," *Sens. Actuators A*, Doi:10.1016/j.sna.2007.02.019.

[7] V. Carvalho, P. Cardoso, M. Belsley, R. Vasconcelos, and F. Soares, "A new statistical reference method for yarn hairiness quantification," presented at the ISIE 2007, Vigo, Spain, Jun. 4–7, 2007.

[8] V. Carvalho, P. Cardoso, M. Belsley, R. Vasconcelos, and F. Soares, "Optical yarn hairiness measurement system," presented at the INDIN 2007, Vienna, Austria, Jul. 23–27, 2007.

[9] V. Carvalho, P. Cardoso, M. Belsley, R. Vasconcelos, and F. O. Soares, "Yarn hairiness characterization using two orthogonal directions," *IEEE Trans. Instrumentation and Measure.*, Doi: 10.1109/TIM.2008.2005082.

[10] J. W. Goodman, *Introduction to Fourier Optics*. New York: McGraw-Hill, 1996.

[11] E. G. Steward, *Fourier Optics: An Introduction*. New York: Dover Publications, 2004.

[12] P. M. Duffieux, *The Fourier Transform and its Applications to Optics*, 2nd ed. New York: Wiley, 1983.

[13] C. K. Madsen, *Optical Filter Design and Analysis: A Signal Processing Approach*. New York: Wiley, 1999.

[14] S. Franco, *Design with Operational Amplifiers and Analog Integrated Circuits*, 3rd ed. New York: Mc-Graw Hill, 2001.

[15] B. Saleh and M. Teich, *Fundamentals of Photonics*. New York: Wiley, 1991.

[16] L. Mandel and E. Wolf, *Optical Coherence and Quantum Optics*. Cambridge, U.K.: Cambridge Univ. Press, 1995.

[17] A. Siegman, *Lasers*. Sausalito, CA: Univ. Science Books, 1986.

[18] Uster Statistics 2007.

[19] Zweigle Product Catalog 2007–2008.

[20] M. Castro and M. Araújo, *Manual de Engenharia Têxtil*. Lisbon, Portugal: Gulbenkian, 1986, vol. II.

[21] V. Carvalho, R. Vasconcelos, F. O. Soares, and M. Belsley, "A comparative study between two yarn diameter and mass variation measurement systems – Capacitive and optical sensors," *Indian J. Fibres Textile*, vol. 33, pp. 119–125, Jun. 2008.

[22] A. Sparavigna, E. Broglia, and S. Lugli, "Beyond capacitive systems with optical measurements for yarn evenness evaluation," *Mechatronics*, vol. 14, no. 10, pp. 1183–1196, Dec. 2004.

[23] M. Norusis, *SPSS 15.0 Guide to Data Analysis*. Englewood Cliffs, NJ: Prentice-Hall, 2007.

Vítor H. Carvalho received the Degree in industrial electronics engineering in the option of telecommunications and industrial informatics in 2002, and the M.Sc. degree in industrial electronics in the option of automation and robotics in 2004, both from Minho University, Guimarães, Portugal. In July, 2008, he received the Ph.D. degree in industrial electronics, which covers the subject presented in this paper.

He is currently working as an Assistant Professor at the Polytechnic Institute of Cávado and Ave (IPCA), Barcelos, Portugal, and in the Portuguese Catholic University (UCP), Braga, Portugal. His main fields of interest are data acquisition, signal processing and industrial informatics.

Paulo J. Cardoso received the Degree in applied physics in 2002 and the M.Sc. degree in biomedical engineering in 2008 from Porto University, Porto, Portugal. He is currently working towards the Ph.D. degree in physics at the Department of Physics (DF), Minho University, Braga, Portugal.

His main fields of interest are the optical signal processing and nonlinear optics.

Michael S. Belsley received the Ph.D. degree in physics from the University of Colorado, Boulder, in 1986.

He then worked at the California State University, Long Beach, Oxford University, and the University of Oregon before joining Minho University, Braga, Portugal, where he has lectured as an Associate Professor of Physics since 1992. His main fields of interest are laser spectroscopy and nonlinear optics.

Rosa M. Vasconcelos received the Degree in textile engineering in 1984 from Minho University, Guimarães, Portugal. In 1993, she received the Ph.D. degree in engineering-textile technology and chemistry on the specialty of textile technology from Minho University.

Since 2005, she has been working as an Associate Professor in the Textile Engineering Department of Minho University. Her fields of interest are textile processes and industrial automation.

Filomena O. Soares received the Degree in chemical engineering in 1986 from Porto University, Porto, Portugal. In 1997, she received the Ph.D. degree in chemical engineering from Porto University.

Since 2007, she has been an Associate Professor in the Industrial Electronics Department, Minho University, Guimarães, Portugal. Her fields of interest are process modeling and control and process automation.